In Situ Scanning Tunneling Microscopy for Platinum Surfaces in Aqueous Solutions

Kingo Itaya,* Shizuo Sugawara, and Katsutoshi Higaki

Department of Engineering Science, Faculty of Engineering, Tohoku University, Sendai 980, Japan
(Received: February 9, 1988; In Final Form: April 19, 1988)

An in situ scanning tunneling microscope was applied for platinum (Pt) surfaces in aqueous solutions. Pt particles, electrodeposited on a highly ordered pyrolytic graphite, were investigated in detail. It was revealed that the shape of the Pt particle was not a smooth semisphere. There were many irregular dislocations such as steps and boundaries. Pt whiskers were also observed. The in situ measurement of Pt electrodes was carried out before and after an electrochemical activation in an aqueous solution of sulfuric acid. Large changes in the surface structure were induced by an electrochemical activation procedure. Very regular parallel-terrace structures appeared, suggesting that the migration of adatoms of Pt produced by the oxidation and reduction cycles should occur toward a particular crystallographic direction. Semispherical domains were observed at different portions of the surface. It was concluded that different morphologies appearing at different points were probably caused by the orientation of each small single crystal composed in the sample.

Introduction

The scanning tunneling microscope (STM) has been finding enormous application fields for topographic imaging and analysis of surfaces in various environments.[1-4] Atomic resolution has been achieved in the imaging of surface reconstructions of Si(111) in ultrahigh vacuum (UHV).[1] However, recent papers have shown that atomic resolution is also obtainable with STM for the samples immersed in aqueous solutions of electrolytes.[5-8]

Electrochemically deposited gold (Au) and silver (Ag) have been investigated in an electrochemical cell by Hansma, et al.[5,6] Our recent paper reported preliminary results of an STM study of platinum (Pt) particles electrodeposited on a graphite electrode in sulfuric acid.[8] Bard et al. described an STM apparatus and observed a test integrated circuit overlaid with Pt in aqueous solutions.[9] These results indicate strongly that in situ STM in solutions is a powerful tool for the examination of electrode surfaces.

The importance of the characterization of electrode surfaces is well recognized in electrochemistry. Among various kinds of electrode materials, platinum is one of the most extensively studied in both technological and fundamental aspects. It is well-known that the highly dispersed Pt catalyst has been widely employed as the air cathode in the phosphoric acid fuel cell.[10-12] With respect to fundamental aspects, the electroadsorptions and desorptions of hydrogen and oxygen on single-crystal Pt surfaces have been investigated by various workers to characterize the effect of surface structure.[13-20]

To understand electrochemical reactions in these systems at the atomic level requires a new method of following the changes in the atomic structure of the electrode surface. UHV techniques, such as low-energy electron diffraction (LEED), have been frequently employed for the characterization of the electrode surface.[14-16] However, it has been pointed out that well-characterized single-crystal surfaces prepared in UHV are easily contaminated during the transfer of samples into the electrochemical environment.[20]

Vázquez et al. have recently described an ex situ observation of the topography of electrochemically activated Pt electrodes in air.[21,22] Fan and Bard have examined Pt electrodes in air and water after different pretreatments.[23]

However, it is reasonable to expect that in situ STM should applicable to an understanding of what happens on Pt electrodes in liquid phases at the atomic level.

In the former part of this paper, we show a detailed in situ STM investigation of fine structures of semispherical Pt particles deposited on a highly ordered pyrolytic graphite (HOPG) electrode. In the latter part, we report, for the first time, an in situ observation of the surface of Pt electrodes activated by electrochemical potential cycles in sulfuric acids.

Experimental Section

Apparatus. Figure 1 shows an illustrative depiction of the microscope (A) and electrochemical cell (B) used for this study. The microscope uses three orthogonal pairs of piezoelectric tubes (Tokin Co., N-21, 3 × 3 × 20 mm) in a three-axis micropositioner. The thumbscrew is the coarse adjustment that allows the sample surface to be brought to within 5-10 μm of the tip under the observation of an optical microscope. A differential micrometer (Mitsutoyo Co., MHF2-13) attached to a spring plate is used to bring the sample within the tunneling range of the tip. The ratio of the vertical motion of the micrometer to that of the sample was about 50, depending on the position of the sample on the spring plate.

The feedback control electronics is functionally similar to that reported in the literature.[24] Burr-Brown high-voltage operational amplifiers (3583) were used as the voltage supplier for the piezoelectric tubes.

The electrochemical cell (Figure 1B) made of a Teflon rod is a three-electrode type with a bright Pt quasi-reference and Pt counter-electrodes. An O-ring is used between the cell and the sample electrode. The cell is firmly held on the spring plate by

(1) Binnig, G.; Rohrer, H. *IBM J. Res. Dev.* **1986**, *30*, 355-369.
(2) Quate, C. F. *Phys. Today* **1986**, *39*, 26-33.
(3) García, N. *Surf. Sci.* **1987**, *181*, 1-412.
(4) Binnig, G.; Rohrer, H.; Gerber, Ch.; Weibel, E. *Phys. Rev. Lett.* **1982**, *49*, 57-61.
(5) Schneir, J.; Sonnenfeld, R.; Hansma, P. K.; Tersoff, J. *Phys. Rev. B* **1986**, *34*, 4979-4984.
(6) Drake, B.; Sonnenfeld, R.; Schneir, J.; Hansma, P. K. *Surf. Sci.* **1987**, *181*, 92-97.
(7) Sonnenfeld, R.; Schardt, B. C. *Appl. Phys. Lett.* **1986**, *49*, 1172-1174.
(8) Itaya, K.; Sugawara, S. *Chem. Lett.* **1987**, 1927-1930.
(9) Liu, H. Y.; Fan, F. F.; Lin, C. W.; Bard, A. J. *J. Am. Chem. Soc.* **1986**, *108*, 3838-3839.
(10) Sarangapani, S.; Akridge, J. R.; Schumm, B. *The Electrochemistry of Carbon*; The Electrochemical Society: Pennington, 1984.
(11) Yeager, E. *J. Electrochem. Soc.* **1981**, *128*, 160C-171C.
(12) Cox, D. F.; Hoflund, G. B.; Laitinen, H. A. *Langmuir* **1985**, *1*, 269-273.
(13) Conway, B. E. *Prog. Surf. Sci.* **1984**, *16*, 1-138, and references theirin.
(14) Hubbard, A. T. *Acc. Chem. Res.* **1980**, *13*, 177-184.
(15) Homa, A. S.; Yeager, E.; Cahan, B. D. *J. Electroanal. Chem.* **1983**, *150*, 181-192.
(16) Wagner, F. T.; Ross, Jr., P. N. *Surf. Sci.* **1985**, *160*, 305-330.
(17) Clavilier, J.; Faure, R.; Guinet, G.; Durand, R. *J. Electroanal. Chem.* **1980**, *107*, 205-209.
(18) Clavilier, J.; Durand, R.; Guinet, G.; Faure, R. *J. Electroanal. Chem.* **1981**, *127*, 281-287.
(19) Clavilier, J.; Armand, D.; Wu, B. L. *J. Electroanal. Chem.* **1982**, *135*, 159-166.
(20) Motoo, S.; Furuya, N. *J. Electroanal. Chem.* **1984**, *172*, 339-358.
(21) Vázquez, L.; Gómez, J.; Baró, A. M.; García, N.; Marcos, M. L.; Velasco, J. G.; Vara, J. M.; Arvia, A. J.; Presa, J.; García, A.; Aguilar, M. *J. Am. Chem. Soc.* **1987**, *109*, 1730-1733.
(22) Gómez, J.; Vázquez, L.; Baró, A. M.; García, N.; Perdriel, C. L.; Triaca, W. E.; Arvia, A. J. *Nature (London)* **1986**, *323*, 612-614.
(23) Fan, F. F.; Bard, A. J., submitted for publication in *Anal. Chem.*
(24) Drake, B.; Sonnenfeld, R.; Schneir, J.; Hansma, P. K.; Slough, G.; Coleman, R. V. *Rev. Sci. Instrum.* **1986**, *57*, 441-445.

0022-3654/88/2092-6714$01.50/0

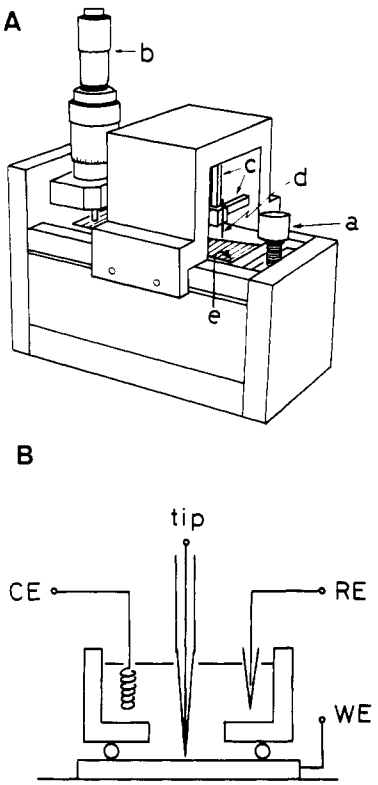

Figure 1. Schematic depictions of the STM apparatus (A) and the electrochemical cell (B). (A) a, thumbscrew; b, differential micrometer; c, piezotubes; d, tip; e, spring plate. (B) WE, working electrode; RE, reference electrode; CE, counterelectrode.

screws. The tunneling tip is a glass-covered Pt electrode. Pure Pt wire (99.99%) with a diameter of 65 μm was directly sealed into a pipette that was pulled on a conventional puller by using thin-walled soft-glass tubing (i.d. = 1 mm, o.d. = 1.6 mm).[25] The thickness of the glass layer of the tip was about 50 μm near the end of Pt wire. The last 20–30 μm of the tip was simply exposed by a turning on a lathe. The tip electrode was sonicated in concentrated sulfuric acid for 1 h before use. Note that the residual current (electrochemical background current) should be less than the tunneling current for the STM measurement. We preexamined the residual current of all tips by cyclic voltammetry in a 0.1 M H_2SO_4 solution. It was found that the residual current level for well-sealed tips showed only 0.2–0.3 nA at a scan rate of 1 mV/s in a potential range between −0.1 and 1 V versus a saturated calomel electrode (SCE). A typical tunneling current employed in this study was 4–5 nA, so that the residual current was only about 5% of the total tunneling current.

Electrochemical measurements were performed with a PAR Model 173 potentiostat. A PAR Model 113 low-noise preamplifier was used for the measurement of the residual current of the tip as described above.

The morphology of electrodeposition of Pt was also examined by a scanning electron microscope (SEM, Hitachi Model H-8010).

Procedure. The electrodeposition of Pt on the basal plane of HOPG (Union Carbide Co.) was carried out by cyclic voltammetry (CV) in a freshly prepared solution of K_2PtCl_6 in 0.1 M H_2SO_4, the same method as reported in the previous paper.[26]

For investigation of Pt surfaces, a bright Pt plate was mechanically polished by using successively finer grades of alumina down to 0.1 μm. The mechanically polished Pt plate was then annealed in a gas-oxygen flame near 1100–1200 °C for 1 h. After this prolonged annealing, the crystal grains could be seen under an optical microscope, suggesting that the Pt sample could be classified as a well-crystallized polycrystalline Pt. The final surface treatment for both the STM and electrochemical observations was carried out by following a procedure employed for electrochemical studies of single crystals of Pt described by Clavilier et al.[17-19] and Motoo and Furuya.[20] The Pt was annealed in a gas-oxygen flame near 1100 °C for 1 min and then quickly brought in contact with ultrapure water (Millipore Q) saturated with hydrogen.

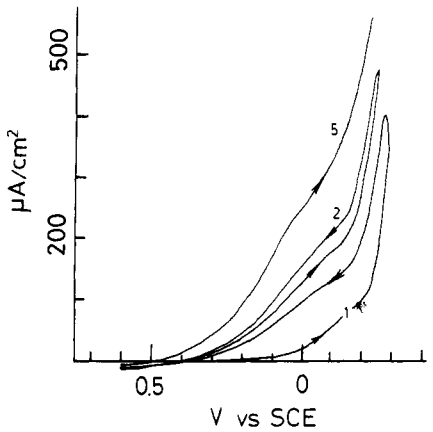

Figure 2. Cyclic voltammograms recorded continuously at a HOPG electrode in a 0.1 M H_2SO_4 solution under nitrogen atmosphere. The numbers on the curves are the repeated cycles at a scan rate of 50 mV/s.

Results and Discussion

Electrodeposition of Pt on HOPG. Figure 2 shows typical CV curves obtained on a basal plane of freshly cleaved HOPG electrode in a 0.1 M H_2SO_4 solution of 5 mM K_2PtCl_6. In the first negative scan from 0.6 V versus SCE, the current due to the reduction of $PtCl_6^{2-}$ commenced at about 0 V and was largely enhanced in the reverse scan. Larger currents were observed in the following potential scans where the current commenced at about 0.4 V versus SCE. These results are basically the same as those obtained on a glassy carbon (GC) electrode described in the previous paper.[26] The reduction current observed in Figure 2 is due to the following reaction:[27]

$$Pt^{IV}Cl_6^{2-} + 4e^- \rightarrow Pt + 6Cl^- \quad (1)$$

The large overpotential observed in the first potential scan is probably due to the formation of Pt nuclei on the basal plane of HOPG. After the formation of these nuclei, the electrodeposition of Pt occurs on the Pt nuclei at lower negative potentials. The behavior shown in Figure 2 is a typical example of the nucleation and growth of the electrodeposition.[27] Note that the onset potential (0 V) is more negative than that (0.2 V) observed on a GC electrode previously.[26] This negative shift of the onset potential is probably due to the perfectness of the basal plane of HOPG. The nucleation of Pt needs larger overpotentials on the HOPG than on a GC electrode.

On the basis of the result shown in Figure 2, a potential program was employed for the electrodeposition as follows: the potential limits for the first cycle were 0.6 and −0.25 V versus SCE and 0.6 and 0.1 V versus SCE for successive potential cycles. Under these limited conditions, nucleation of Pt can be expected to occur only in the first potential cycle and Pt particles to grow in successive scans. The loading level of Pt on the HOPG electrode was calculated from the charge consumed in the repeated potential scans, assuming current efficiency to be unity under the limited potential scan described above.

We first describe the morphology of the Pt particles observed by a SEM. Typical SEM micrographs of Pt particles on the HOPG with a loading level of 20 mC/cm² (10 μg/cm²) are shown in Figure 3. As can be seen, the Pt particles are almost semispherical and randomly distributed on the basal plane of HOPG. The diameter of the semispherical Pt particle seems to be of the order of 1500–2000 Å for the sample shown in Figure 3. The distribution of the size of the particles seems to be fairly narrow because the nucleation of Pt occurred only in the first potential

(25) Merrill, E. G.; Ainsworth, A. *Med. Biol. Eng.* **1972**, *10*, 662–672.
(26) Itaya, K.; Takahashi, H.; Uchida, I. *J. Electroanal. Chem.* **1986**, *208*, 373–382.
(27) Feltham, A. M.; Spiro, M. *Chem. Rev.* **1971**, *71*, 177–193.

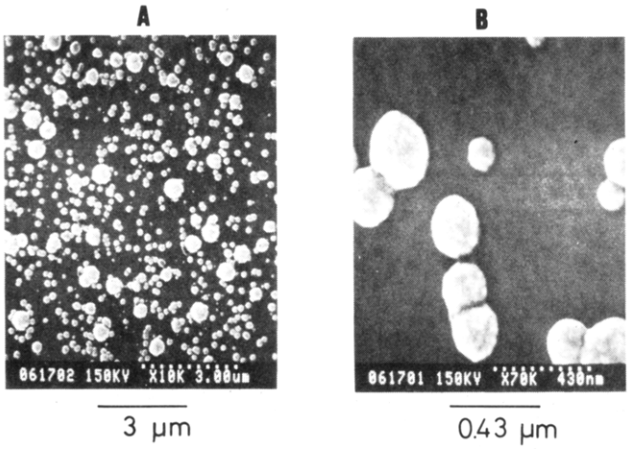

Figure 3. Scanning electron micrographs of Pt particles on a HOPG electrode with a loading level of 20 mC/cm^2.

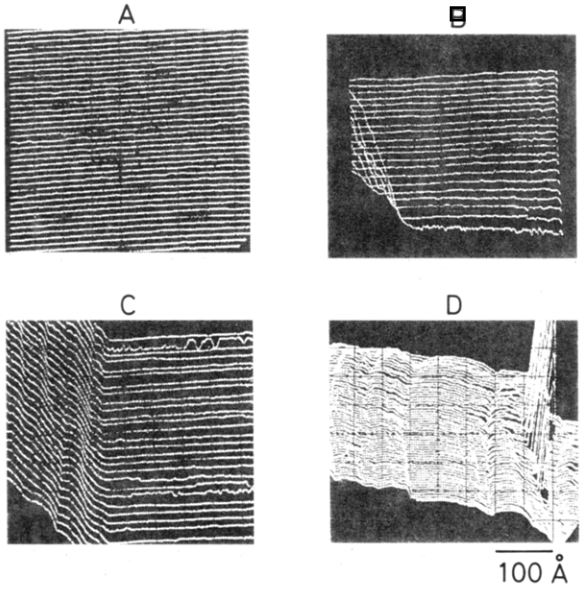

Figure 4. STM images in a 0.1 M H_2SO_4 solution of a HOPG surface after 20 mC/cm^2 of Pt was electrodeposited. The tunneling current was 4 nA. The tip was 100 mV with respect to the graphite. The x, y, and z scales are all the same.

scan. Note that the sample shown in Figure 3 was investigated under the SEM observation after the examination of STM in a sulfuric acid solution, as will be discussed in the following section.

After the electrodeposition of the loading level of 10 μg of Pt/cm^2 in the chloroplatinate solution, the electrochemical cell was disconnected from the potentiostat, and the chloroplatinate solution was replaced with a 0.1 M H_2SO_4 solution. Hansma and Sonnenfeld have used a platinum–iridium tip even in plating solutions for imaging the surfaces of electrodeposited Au[6] and Ag[7]. The question is raised, however, whether the electrodeposition on the tunneling tip might not have occurred during the observation of STM. We believe that the replacement of the chloroplatinate solution by pure H_2SO_4 is necessary to avoid the deposition of Pt on the Pt tip used here. After the complete replacement of the solution, the STM feedback circuit (Z direction) was reconnected between the tip and HOPG electrodes. During the STM measurement, the reference and counterelectrodes shown in Figure 1B were not used.

Figure 4 shows a series of STM images of the HOPG electrode with the loading level of 20 mC/cm^2. Figure 4A, taken on a bare HOPG where no Pt particles were observed, shows a perfectly flat surface under this magnification. When the position of the tip was shifted to the left-hand side of Figure 4A, applying a bias voltage to the x piezotube, an edge of a single Pt particle clearly appeared in the left corner in Figure 4B. A further shift in the position of the tip made it possible to image an edge of the sem-

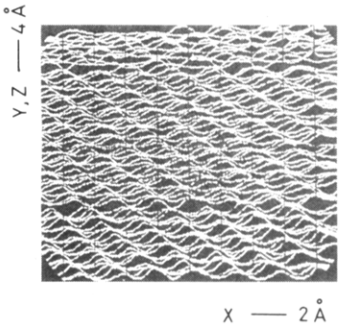

Figure 5. STM image of the surface of graphite obtained at the flat region shown in Figure 4A. The tunneling current and voltage were the same as indicated in Figure 4.

ispherical Pt particle existing on a near-to-atomically flat surface of HOPG as shown in Figure 4C. Figure 4D was taken with atomic resolution on almost the top of the Pt particle after settling a thermal drift. It is now easily seen that the shape of the Pt particle is not a completely smooth semisphere as expected by the SEM observation. There are many irregular dislocations such as steps and boundaries (2–20 Å in heights), which must have been formed during electrodeposition under the procedure described above. In addition to these structures, two or three needles can be seen on the right-hand side of Figure 4D. Their sizes were ca. 100–200 Å in height and 10–20 Å in diameter. It is reasonable to assume that these needles are Pt whiskers existing on the Pt particles. Note that the size of whiskers estimated from the image shown in Figure 4D seems to be more apparent than real. STM images depend on sample surface and tip topographies. It is suggested that a predetermined tip geometry is important for high-resolution imaging of nonperiodic surface features of unknown size.[1] However, it might be very difficult to characterize the tip geometry in an atomic scale for in situ STM studies in electrolyte solutions.

Under observation with higher magnifications at the flat region as shown in Figure 4A, an atomic corrugation due to the graphite structure could be observed in the same sulfuric acid solution, as shown in Figure 5. The observed structure is quite similar to that obtained in liquids by previous works.[5,7,8] The result shown in Figure 5 indicates strictly that neither a single adatom nor a cluster exists in these flat regions. However, some parts of the apparently flat surface of HOPG, particularly in the vicinity of Pt particles, showed noisy signals in the tunneling current. This behavior might be due to the existence of very small Pt particles (clusters). Attempts to image these ultramicro particles of Pt have not yet been successful, because the density of these particles was quite small in the sample examined here. However, the size of the particle can be dramatically reduced under carefully controlled electrochemical conditions for the electrodeposition of Pt. The direct observation of the nucleations is now of special interest. Experiments on this line are currently under way.

Platinum Electrodes in Sulfuric Acid. STM has been already applied for clean Pt surfaces in UHV. On the other hand, Vázquez et al. have recently described an ex situ observation in air of the topography of electrochemically highly activated Pt electrodes.[21,22] Fan and Bard have recently examined Pt electrodes in air and water after different pretreatments.[23] However, application of the in situ STM to electrodes in aqueous solutions promises to give information more useful for an understanding of the electrochemical reactions occurring on Pt electrode surfaces.

The final surface treatment was carried out following the procedure described above. Figure 6 shows the typical cyclic voltammograms of the Pt electrode obtained in a 0.1 M H_2SO_4 solution. Curve A was measured when the positive potential was limited in the double-layer region. The electrode potential was scanned between 0.4 and −0.23 V versus SCE, where hydrogen adsorption and desorption peaks only were observed. Identical voltammograms in shape and height were recorded after the potential cycles for 30 min or even more, indicating that the Pt surface has been maintained clean from the beginning of the

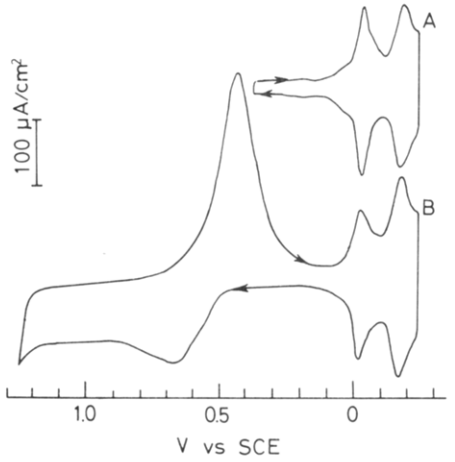

Figure 6. Cyclic voltammograms of a polycrystalline Pt surface in a 0.1 M H_2SO_4 solution. The scan rate was 100 mV/s. Curve A: the electrode potential was scanned between 0.4 and −0.23 V versus SCE after flame treatment. Curve B: after 50 cycles between 1.28 and −0.25 V versus SCE at a scan rate of 200 mV/s.

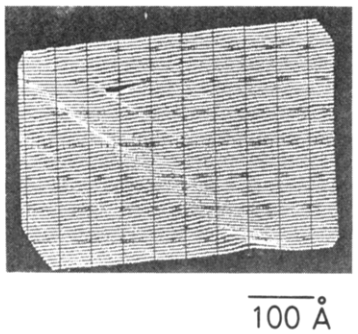

Figure 7. STM images in a 0.1 M H_2SO_4 solution of a polycrystalline Pt surface after flame treatment. The tunneling current, 6 nA; the tip: 90 mV. The x, y, and z scales are the same as indicated.

potential cycles. The amount of hydrogen adsorbed on the Pt surface is calculated as ca. 0.21 ● 0.02 mC/cm² by an integration of the reduction peaks showed in Figure 6. This value is almost identical with a value calculated for a polycrystalline Pt surface (0.18 mC/cm²).[28] The above results are sufficient proof that the Pt surface produced by the present procedure is clean and probably flat on an atomic scale. Curve B in Figure 6 was recorded after 50 cycles between the electrode potentials (−0.25 and 1.28 V) at which hydrogen and oxygen are slightly evolved. The above potential cycling is a commonly used procedure for the activation of Pt electrodes. The shape of the voltammogram (Figure 6B) seems to be typical for polycrystalline Pt electrodes. The actual surface area of the Pt electrode was slightly increased only about 10% after the 50 potential cycles. Arvia et al. applied repetitive square-wave potential cycles between 0 and 2.3 V to polycrystalline Pt.[29,30] Application of such an unusually high anodic potential causes a very large increase in the surface area as in the case of platinum black.[21,22] However, the increase in the surface area caused by the much more mild activation procedure employed in this study is quite small as shown in Figure 6B.

On the basis of the above electrochemical study, the in situ observation of Pt electrodes was carried out before and after the electrochemical activation in the same 0.1 M H_2SO_4 solution. Exactly the same gas-oxygen flame final surface treatment was employed for STM observation.

Figure 7 shows a typical image of the virgin Pt surface (unactivated) observed in a 0.1 M H_2SO_4 solution. Near-to-

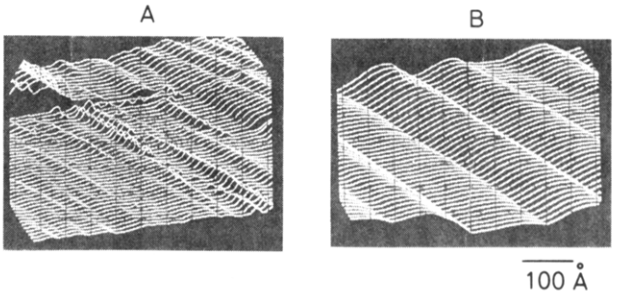

Figure 8. STM images of a Pt surface after 50 cycles between 1.28 and −0.25 V versus SCE. The tunneling current, 6 nA; the tip, 90 mV.

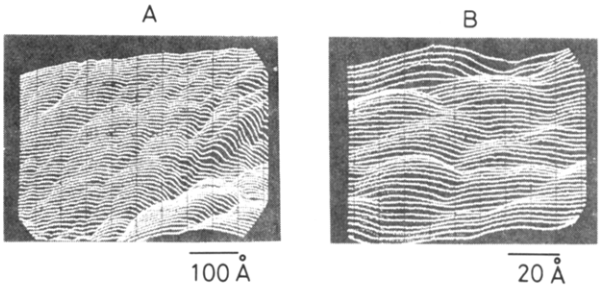

Figure 9. STM images at different locations. The tunneling current, 6 nA; the tip, 80 mV.

atomically flat surfaces were observed with a few shallow multiatomic steps (1–20 Å in height) for all views with different positions. This indicates directly that the annealing procedure in a gas-oxygen flame produces near-to-atomically flat surfaces consistent with the result discussed above. The tunneling current was fairly stable as long as the Pt surface was kept clean. However, it was found that the current became sometimes noisy for different samples. Such noisy signals in the tunneling current are probably caused by a surface contamination. In contrast with the result shown in Figure 7, Vázquez et al. reported more irregular structures for untreated Pt specimens observed in air.[21] It is suggested by Fan and Bard that such differences might be due to the difference in the pretreatment.[23]

After observations of STM images at near the area shown in Figure 6, the electrode potential of the Pt specimen was cycled for 50 times at a scan rate of 0.2 V/s between the potentials of −0.25 and 1.25 V. During the potential cycling, the tunneling tip was retracted only about 2000–3000 Å from the surface and disconnected from the STM feedback circuit. It was made sure in a separate experiment that such a small retraction did not cause a large change in the relative position of the tip to a particular point on the surface of the sample, during the potential cycles employed here.

Figure 8 shows STM images obtained after the electrochemical activation described above. These images were obtained near the area shown in Figure 7. It can be surprisingly seen that large changes are induced by the electrochemical activation procedure. Relatively smooth terraces spaced in the order of 5–20 Å and parallel ridges are clearly observed in Figure 8A. Another image, shown in Figure 7B, was obtained near the area depicted in Figure 8A. In this case, very regular parallel-terrace structures separated by ca. 150 Å appear. Such reconstructed surfaces must be produced by the surface migration of adatoms of Pt produced by the oxidation and reduction cycles under the potential cycles described above.

It should be particularly pointed out that the direction of the steps, ridges, and terraces observed in Figure 8, parts A and B, is exactly the same as that of the shallow atomic steps observed for the unactivated Pt surface shown in Figure 7. This coincidence in direction is very important for the direction of the migration of adatoms of Pt. We believe that the migration of Pt adatoms must occur toward a direction perpendicular to that of the shallow steps appearing on the unactivated Pt surface, yielding the reconstructed surfaces shown in Figure 8. Similar ridges have been reported in air after applying a large anodic potential.[21,22]

(28) Spenadel, L.; Boudart, M. *J. Phys. Chem.* **1960**, *64*, 204–207.
(29) Cervino, R. M.; Triaca, W. E.; Arvia, A. J. *J. Electrochem. Soc.* **1985**, *132*, 266–267.
(30) Cervino, R. M.; Triaca, W. E.; Arvia, A. J. *J. Electroanal. Chem.* **1985**, *182*, 51–60.

However, it is very surprising to observe such a large change in morphology under the potential cycles applied in this study. As discussed before, the total surface area of the Pt after the 50 potential cycles increased only about 10% of that for the virgin surface.

We have carried out similar observations at different portions of the specimen. Another typical structure we observed is shown in Figure 9. In this case, parallel ridges were not clearly observed. Instead of the parallel regular structures shown in Figure 8, semispherical domains have predominantly been observed. The diameter and height of the semispheres are in a range of ca. 50 and 10 Å, respectively. Similar semispherical domains, namely, domelike or pebblelike, structures were also distinguished in air.[21,23]

Different morphologies observed at different points are probably caused by the crystallographic orientation of each small single crystals composed in the specimen.

We are currently carrying out experiments on Pt single crystals. Similar semispherical domains have been found on the Pt(111) single crystal after electrochemical activation.[31] Wagner and Ross have recently investigated the structures formed by oxidation-reduction cycling of Pt(111) surface in aqueous solutions using LEED analysis.[16] They suggested that a randomly stepped surface was formed at higher anodic potentials in HF solutions. Such structural changes should be directly determined by the STM method described here.

The results reported in this paper strongly encourage us to explore the applications of STM to the in situ observation of Pt surfaces in electrolyte solutions.

Acknowledgment. We express our thanks to Professor N. Furuya (Yamanashi University) for his guidance of the treatment of Pt and to Professor A. J. Bard (Texas University) for sending us his paper prior to its publication. This work was supported in part by Ministry of Education, Science and Culture, Grant-in-Aid for Special Project Research No. 480540125498.

Registry No. Pt, 7440-06-4; H_2SO_4, 7664-93-9; graphite, 7782-42-5.

(31) Sugawara, S.; Itaya, K., unpublished result, 1987.

Interaction of Surfaces Carrying Grafted Polyelectrolytes

S. J. Miklavic* and S. Marčelja

Department of Applied Mathematics, Research School of Physical Sciences, The Australian National University, Canberra ACT 2601, Australia *(Received: February 12, 1988; In Final Form: June 3, 1988)*

We extend the analytical self-consistent mean-field theory of grafted polymer brushes introduced recently by Milner, Witten, and Cates to cover the cases of polyelectrolyte chains attached to a charged surface in contact with an electrolyte solution. For semidilute chains within the linear Poisson-Boltzmann regime, solutions of the statistical mechanics problem are still analytical, and we can easily explore the behavior of the system as a function of the charge on the polymer, charge on the surface, and electrolyte concentration. The grafted polyelectrolyte chain conformations are sensitive to all of the above parameters, and we present a method for the relevant calculations. It is also simple to evaluate the interaction between surfaces carrying grafted polyelectrolytes, and the resulting behavior is illustrated with examples.

Introduction

Problems involving the interaction of surfaces bearing grafted polyelectrolyte chains are sometimes encountered in studies of polymeric stabilization of colloidal dispersions. While this topic is considered important, it has received relatively little experimental or theoretical attention.[1] At a low ionic strength and a high degree of ionization, the electrostatic stabilization mechanism due to the additional repulsion induced by polyelectrolytes at the surfaces becomes dominant. In comparison with the stabilization by neutral polymers, under such conditions the stability of a colloidal dispersion is increased.

The exterior surfaces of biological cells carry a layer or coating of extended, flexible macromolecules of complex structure, most of which bear a net polyionic charge. This coat, called a glycocalyx, comprises a mixture of glyco(sugar) lipids and glycoproteins and is considered to play an important role in cellular interactions. Consequently, a study of surfaces coated with a layer of polyelectrolytes, either in isolation or interacting, is of particular interest in several biological areas. We have been drawn to the study of this topic by the need to understand the effects on the electrophoretic mobility of cells by changes in the coat structure with changing electrolyte concentration, although this is not explicitly treated here.

The coupling between the response of the grafted polyelectrolyte chains and the surrounding ionic solution to any change in the conditions makes the evaluation of properties of such surfaces difficult. For instance, a self-consistent mean-field calculation (for the case of polyelectrolyte adsorption) has been carried out by Papenhuizen et al.,[2] but this has necessarily involved detailed numerical work.

In this present work, an important recent advance in the understanding of surfaces bearing grafted neutral polymer chains is used to develop analogous analytical methods for similarly attached polyelectrolytes under a variety of different external conditions. As shown by Milner, Witten, and Cates[3] (hereafter this work will be referred to as MWC), at moderate surface concentrations of grafted polymer chains (the semidilute regime), the statistical mechanical properties of the chains can be evaluated by using an analogy with the (classical) mechanics of a particle moving in a mean potential field. This method is readily generalized to the case of charged chains grafted to an arbitrarily charged surface and immersed in an electrolyte solution. The resulting theory can still be solved analytically, and the solutions provide a simple and convenient way to explore the conformations and the interactions of such surfaces as the polymer charge, surface charge, and electrolyte concentration are varied. In the following sections we consider in turn the extension of the method to charged chains, the calculated density profiles and surface interactions, and the region of applicability of the resulting method.

Method

The method utilizes a polymer description based on an analogy with classical mechanics.[4] It is a mean-field approximation, valid

(1) Napper, D. H. *Polymer Stabilization of Colloidal Dispersions*; Academic: New York, 1986.

(2) Papenhuizen, J.; van der Schee, H. A.; Fleer, G. J. *J. Colloid Interface Sci.* **1985**, *104*, 540.

(3) Milner, S. I.; Witten, T. A.; Cates, M. E. *Europhys. Lett.*, **1988**, *5*, 413; *Macromolecules*, in press.

0022-3654/88/2092-6718$01.50/0